AIMS Mathematics, 7(5): 8263–8289.
DOI: 10.3934/math.2022461
Received: 30 November 2021
Revised: 03 February 2022
Accepted: 08 February 2022
Published: 25 February 2022

http://www.aimspress.com/journal/Math

Research article

Low-cost adaptive fuzzy neural prescribed performance control of strict-feedback systems considering full-state and input constraints

Yankui Song[1,2], Bingzao Ge[3], Yu Xia[1,2], Shouan Chen[1,*], Cheng Wang[1,2] and Cong Zhou[1,2]

[1] State Key Laboratory of Mechanical Transmission, Chongqing University, Chongqing 400044, China
[2] College of Mechanical Engineering, Chongqing University, Chongqing 400044, China
[3] Zhejiang Jinfei Kaida Wheel Co., Ltd., Jinhua 321000, China

* **Correspondence:** Email: 20190701144@cqu.edu.cn; Tel: +8618685438601.

Abstract: A low-cost adaptive neural prescribed performance control (LAFN-PPC) scheme of strict-feedback systems considering asymmetric full-state and input constraints is developed in this paper. In the controller design procedure, one-to-one nonlinear transformation technique is employed to handle the full-state constraints and prescribed performance requirement. The Nussbaum gain technique is introduced for solving the unknown control direction and the input constraint nonlinearity simultaneously. Furthermore, a fuzzy wavelet neural network (FWNN) is utilized to approximate the unknown nonlinearities. Compared with traditional approximation-based backstepping schemes, the constructed controller can not only overcome the so-called "explosion of complexity" (EOC) problem through command filter, but also reduce filter errors by error compensation mechanism. Moreover, by constructing a virtual parameter, only one parameter is required to be updated online without considering the order of system and the dimension of system parameters, which significantly reduces the computational cost. Based on the Lyapunov stability theory, the presented controller can ensure that all the closed-loop signals are ultimate boundedness, and all state variables and tracking error are restricted in the prespecified regions. Finally, the simulation results of comparison study verify the effectiveness of the constructed controller.

Keywords: adaptive control; prescribed performance; command filter; full-state constraints; input constraint; low-cost
Mathematics Subject Classification: 93B52, 93C95, 93D05

1. Introduction

The control problems of nonlinear systems have received a great deal of attention, and a considerable amount of literatures have been published [1–5]. A two-layer neural networks (NNs) based robust control for nonlinear induction motors is proposed in [1]. In [2] the unknown nonlinear items in the dynamic model of robotic manipulators are identified by NNs. Dynamic properties and optimal stabilization issues of fractional-order (FO) self-sustained electromechanical seismograph system is investigated in [3]. A neural adaptive control scheme is raised for a class of uncertain multi-input/multi-output nonlinear systems [4] and only one learning parameter is updated in the parameter identification. And coupled FO chaotic electromechanical devices are studied in [5]. Specifically, an adaptive dynamic programming policy is proposed to address the zero-sum differential game issue in the optimal neural feedback controller. Obviously, approximation-based adaptive backstepping control has been widely utilized in designing controllers for various nonlinear systems [6–8]. However, traditional approximation-based adaptive backstepping technique faces two crucial issues that hinder its application. The first issue is so-called "EOC" arising from the derivations of virtual control input [7]. The second one is a large computational burden caused by high precision approximation requirements [8].

For the backstepping technique, the design of the control law relies on intermediate state variables as virtual control signals. The controller of each subsystem requires the virtual control signal and its derivative. The lower-order derivatives of the virtual control signals are likely simple in theory, but the higher-order derivatives in higher-order systems are quite complex, which is called the "EOC" problem. For handling the "EOC" problem, a first-order filter was used to calculate the virtual control signal derivatives in each recursive step [9]. This technique is the so-called dynamic surface control (DSC). The utilization of the first-order filter overcomes the EOC problem, but its own characteristics lead to the derivative errors of virtual control signal, which will certainly affect the tracking performance of the system. Based on this, a modified scheme of the DSC method named command filter based control (CFC) method was proposed in [10]. On the one hand, the EOC problem is avoided by substituting a first-order filter with a second-order one to obtain the derivatives of the virtual control signal. On the other hand, the filter errors are compensated by a constructed error compensation mechanism for obtaining better tracking performance of the system. Moreover, constructing an effective error compensation mechanism needs to be further studied.

For the approximation-based control, the NNs or fuzzy logic systems (FLSs) are utilized to approximate unknown functions and external disturbances for ensuring better tracking performance [11,12], which is also a kind of learning control [13]. In [11] a NNs-based approximator is utilized to solve the unmodeled dynamics of the system. FLSs are employed to identify unknown functions existing in systems [12]. Iterative learning control schemes are designed to suppress the vibrations in bending and twisting of the flexible micro aerial vehicle [13]. The approximation accuracy improves with the increase of the number of neural network nodes or fuzzy rules in general, but it also significantly increases the number of estimated parameters. Therefore, the burdens of computation required for online learning will become very heavy. For decreasing the computational burden of approximation-based control, a tuning-function is inserted in the controller of strict-feedback systems [14,15], in which the number of parameter to be updated is the same as the number of unknown parameters. Recently, a kind of one-parameter estimation approach is proposed in [16,17], which needs only one parameter to be updated online and can significantly reduce the computational burden. Nevertheless,

the mentioned control schemes do not take issues of input constraints, state constraints and prescribed performance into account. Therefore, for applying to a broader range of control problems with security, reliability and performance consideration in reality, further research is needed.

In the real world, many physical constraints are generated with security and reliability consideration, such as the output of MEMS resonator [18], the state constraint of aircraft engine [19] and the input constraint of magnetic-field electromechanical transducer [20]. Obviously, severe security matters, performance degradation, and other troubles can be caused without considering these constraints. For the issue of input constraint, a considerable amount of literatures have been published about it [21–23]. A non-smooth and piecewise input constraint model is described in [21]. Furthermore, the model in [22] is a smooth but piecewise function. The input constraint nonlinearity is tackled by asymmetric smooth input constraint model in [23]. For the issues of output constraint and state constraint, Barrier Lyapunov Function (BLF) is seen as an effective tool, and a significant number of typical works have been published including symmetric BLF [24,25] and asymmetric BLF [26,27]. However, the aforementioned BLF-based controllers have the following three drawbacks: 1) Discontinuous actions exist when constructing asymmetric BLF deals with asymmetric constraints; 2) Output/state constraints are achieved indirectly through error constraint, which leads to a more conservative initial output and state; 3) It is not allowed to handle both constrained and unconstrained systems without changing the controller structure. Although the integral BLF (IBLF)-based approach is possible to tackle output/state constraints directly [28], it can only overcome the disadvantages 1) and 2). By constructing a novel state transformation nonlinear function in [29,30], all those shortcomings can be overcome simultaneously. However, in practical applications, ensuring system security and reliability is the foundation, and achieving high performance control of the system is surely the ultimate goal. To be the best of our knowledge, no relevant results have been reported which can overcome the all above drawbacks and ensure safety reliability and high performance of systems simultaneously.

In this paper, with consideration of security, reliability and high performance, a LAFN-PPC of strict-feedback systems considering asymmetric full-state and input constraints is raised. In the controller design procedure, the constrained system is transformed into an unconstrained system using one-to-one nonlinear state transformation technique. One-to-one nonlinear error transformation technique is used to guarantee the prescribed performance. Furthermore, the unknown control direction and the input constraint nonlinearity are resolved by Nussbaum gain technique simultaneously. By introducing command filter and an error compensation mechanism, the constructed scheme can not only overcomes the so-called "EOC" problem, but also reduces filter errors. Moreover, the maximum values of the norm of optimal weight vector in FWNN is constructed as a virtual parameter, and the only one virtual parameter is estimated instead of the optimal weight vectors (OWVs). Regardless of the order of the system and the dimension of the system parameters, only one parameter is required to be updated online, which significantly reduces the computational burdens. The major contributions comparing with the existing ones are listed as:

1) In order to ensure the controlled systems with higher security, faster response speed and lower tracking error simultaneously, we combine a simple state transformation function with an error transformation function. All states and tracking error are always in symmetric or asymmetric prescribed bounds. Compared with the BLF-based methods [24–27], the LAFN-PPC can overcome all the three drawbacks, because we utilize the state transformation function instead of BLF, by which the constrained system is converted to an unconstrained system. In contrast to state transformation based

methods [29,30], the tracking error is always remained within the prescribed performance bound by using an error transformation function.

2) By using command filtering to get the virtual control signal derivatives, the "EOC" problem of traditional backstepping method is overcome, the filter error caused by command filter is compensated by the carefully constructed error compensation mechanism. Compared with [1–5], the method we take only requires the reference signal and its first derivative, which greatly reduces the amount of calculation and meets many practical engineering requirements.

3) To significantly improve the computational efficiency of FWNN-based approximator and to replace estimating the OWVs in each step of backstepping, we construct the maximum value of the norm of OWVs in the FWNN as a virtual parameter. Only one virtual parameter needs to be estimated in the FWNN-based approximator, with this one-parameter estimation-based approach, the number of parameters updated online is independent of the order of the system and the dimension of OWVs, and the computational burden is significantly reduced, while the computational efficiency is significantly improved.

2. System formulation and preliminaries

2.1. System descriptions

The considered strict-feedback systems with input constraint nonlinearity are given as

$$\begin{cases} \dot{x}_i = f_i(\bar{x}_i, \ell_i) + x_{i+1}, & i = 1, \ldots, n-1 \\ \dot{x}_n = f_n(\bar{x}_n, \ell_n) + gu, & u = C(v) \\ y = x_1 \end{cases} \tag{2.1}$$

where $\bar{x}_i = [x_1, \ldots, x_i]^T \in R^i$, $i = 1, \mathrm{K}, n$ and $v \in R$ are the states and the system input. $y \in R$ denotes the system output. $x = [x_1, \ldots, x_n]^T \in R^n$ are the whole states of the system, $f_i(\bar{x}_i, \mathrm{l}_i)$, $i = 1, \ldots, n$ are unknown smooth functions, Specifically, $f_i(\bar{x}_i, \mathrm{l}_i)$ denote system uncertainties and external disturbances, ℓ_i are the unknown constant parameters inseparable from $f_i(\bar{x}_i, \mathrm{l}_i)$. g denotes the unknown control gain. Here, u is the actual control signal which is subjected to the input constraint nonlinearity $C(v): R \to R$. And the input constraint nonlinearity will be given later. In this paper, $x_i(t)$ are constrained in the open sets $(-\underline{\kappa}_i, \bar{\kappa}_i)$, i.e., $x_i(t) \in \Omega_i$.

As is known that input saturation of actuator is a common problem. The input saturation nonlinearity can seriously affect the safety and performance of the system. How to cope with the saturation nonlinearity has become an urgent and challenging research issue. In this paper, we take the input constraint nonlinearity into account. Mostly, the input constraint nonlinearity [21] can be expressed as

$$u = C(v) = \begin{cases} u^-, & v_i < u^-, \\ v_i, & u^- \le v_i \le u^+, \\ u^+, & v_i > u^+, \end{cases} \tag{2.2}$$

where u^+ and u^- are the upper/lower bounds of $u(t)$.

To simplify the design of the control, we can define $\Delta(v) = u - c_v v$, where c_v is a positive

constant. We can rewrite the input constraint model as:

$$u = c_v v + \Delta(v). \tag{2.3}$$

Based on the above strict-feedback systems, the control object of this paper is to design a LAFN-PPC for system (2.1) to realize the following purposes:

(a) All signals of the system are in the sense of uniformly ultimate boundedness.

(b) The input signal and full state variables can be strictly restricted in asymmetric upper and lower bounds.

(c) The output signal can track the reference signal very well. And the output tracking error can be strictly restricted in upper and lower bounds.

2.2. FWNN

The FWNN [20] has strong power in function approximation, which consists of a series of fuzzy IF-THEN rules as:

If Z_1 is M_1^j and … Z_n is M_n^j, then $\hat{f}_s$ is ω_j, $j = 1, \ldots N_s$, where M_i^j, $i = 1, \ldots, n_s$, $j = 1, \ldots, N_s$, is jth member function for ith input, n_s and N_s represent the number of inputs and rulers (fuzzy logical system), respectively.

The FWNN shown in Figure 1 consists of five lawyers, including an input layer, a fuzzification layer, a membership layer, a rule layer, and an output layer. The firing degrees of rulers are defined as

$$\hat{\xi}_i = \sum_{j=1}^{n} \left(1 + \frac{\left(z_i - c_i^j\right)^2}{\omega_i^j}\right) e^{-\frac{\left(z_i - c_i^j\right)^2}{\omega_i^j}},$$

$$\xi_i = \sum_{j=1}^{n} \left(1 - \frac{\left(z_i - c_i^j\right)^2}{\omega_i^j}\right) e^{-\frac{\left(z_i - c_i^j\right)^2}{\omega_i^j}},$$

where $i = 1, \mathrm{K}, N$, $j = 1, \mathrm{K}, n$, n and N denote the number of inputs and rulers (neural network system). c_i^j and ω_i^j represent the center and width of member function.

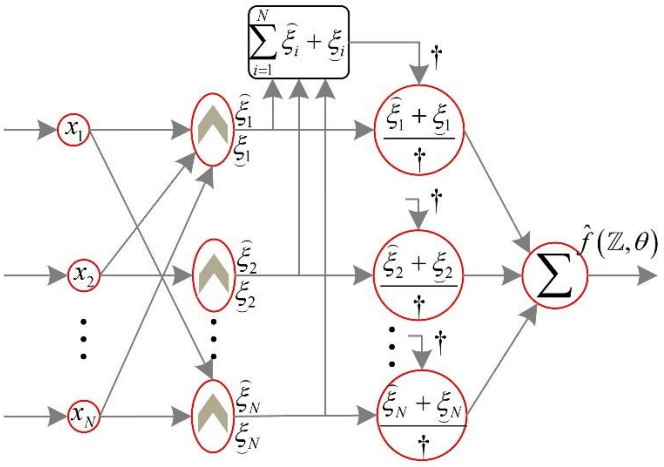

Figure 1. The schematic diagram of the FWN.

The firing degrees are defined as

$$\xi_i = \frac{\overline{\xi}_i + \underline{\xi}_i}{\sum_{i=1}^{N}\left(\overline{\xi}_i + \underline{\xi}_i\right)}, \quad i = 1,\mathrm{K}\,,N\,.$$

The FWNN can be described as

$$f(\theta,\mathbb{Z}) = \theta^T\xi(\mathbb{Z}) + \varepsilon(\mathbb{Z}) \tag{2.4}$$

where $f(\theta,\mathbb{Z})$ is a continuous function which is bounded in closed compact set $\mho \to R^n$, $\mathbb{Z} = [Z_1, Z_2, \cdots, Z_N] \in \mho \subset R^n$ is the input vector, n is the input dimension of neural network. $\theta = \left[\theta_1, \theta_2, \mathrm{L}\ \theta_N\right]^T \in R^N$ denotes the weight vector, and $N > 1$ is the node number of neuron. and $\xi(\mathbb{Z}) = [\xi_1(\mathbb{Z}), \xi_2(\mathbb{Z}), \cdots, \xi_N(\mathbb{Z})]^T \in R^N$ indicates the basic function vector. ε is the estimation error. And there is a positive constant ε_{Mi} which satisfies $\left|\varepsilon_i\right| \le \varepsilon_{Mi}$, $i = 1,\mathrm{K}\,,n$.

Lemma 1 [20]**.** Continuous function $f(\mathbb{Z})$ is defined on a compact set $\mho$. And for $\varepsilon(\mathbb{Z}) > 0$, there is a FWNN satisfying

$$\sup_{x\in\Omega}\left|f(\mathbb{Z}) - \hat{f}(\mathbb{Z},\theta)\right| \le \varepsilon(\mathbb{Z}).$$

The optimal parameter θ^* is equal to $\underset{\theta\in\mho_\theta}{argmin}\left[\sup_{\mathbb{Z}\in\mho}\left|f(\mathbb{Z}) - \hat{f}(\mathbb{Z},\theta)\right|\right]$, where $\mho_\theta$ is a compact set, and $\tilde{\theta} = \theta^* - \theta$, where θ^* represents the estimation of θ.

2.3. State transformation

For resolving physical constraints generated with security and reliability consideration, the following state transformation function [29,30] is introduced to achieve asymmetric constraints, symmetric constraints and no constraints on states simultaneously in a unified form:

$$s_i(t) = \frac{\underline{\kappa}_i\overline{\kappa}_i x_i(t)}{\left(\underline{\kappa}_i + x_i(t)\right)\left(\overline{\kappa}_i - x_i(t)\right)} \tag{2.5}$$

where $\underline{\kappa}_i$ and $\overline{\kappa}_i$ are positive constants, the initial state $x_i(0) \in \Omega_i$, $i = 1,2,\mathrm{K}\,,n$. It is obvious that if the states $x_i(t) \to -\underline{\kappa}_i$ or $x_i(t) \to \overline{\kappa}_i$, the transformed states $s_i(t) \to \pm\infty$. Therefore, the state transformation function can constrain $x_i(t)$ within the open sets $\left(-\underline{\kappa}_i, \overline{\kappa}_i\right)$, i.e., $x_i(t) \in \Omega_i$.

Remark 1. If asymmetric constraints need to be addressed, i.e., let $\underline{\kappa}_i \ne \overline{\kappa}_i$, $i = 1,2,\mathrm{K}\,,n$. Else symmetric constraints need to be tackled, i.e., let $\kappa_i = \underline{\kappa}_i = \overline{\kappa}_i$. Then (2.5) becomes

$$s_i(t) = \frac{\kappa_i^2 x_i(t)}{\kappa_i^2 - x_i^2(t)}. \tag{2.6}$$

If no constraints need to be handled, let $\kappa_i \to +\infty$. It is clear that $s_i(t) \to x_i(t)$, i.e.,

$$\lim_{\kappa_i \to +\infty} s_i(t) = x_i(t). \tag{2.7}$$

The above state transformation function can solve the control problems with asymmetric, symmetric and no state constraints in a unified form. Furthermore, it can handle above three kinds of control problems without changing adaptive laws. Figure 2 shows that the state transformation function can constrain $x_i(t)$ within the open set $(-\underline{\kappa}_i, \bar{\kappa}_i)$ (For the symmetric one: $\underline{\kappa}_i = \bar{\kappa}_i = 4$; For the asymmetric one: $\underline{\kappa}_i = 4$, $\bar{\kappa}_i = 6$).

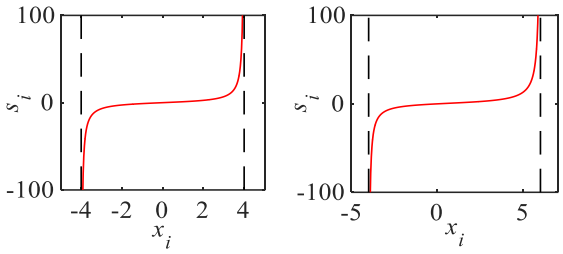

Figure 2. The relationship between s_i and x_i (symmetric and asymmetric form).

The state transformation function can be rewritten as

$$x_i(t) = \eta_i s_i(t) \tag{2.8}$$

where

$$\eta_i = \frac{\left(\underline{\kappa}_i + x_i(t)\right)\left(\bar{\kappa}_i - x_i(t)\right)}{\underline{\kappa}_i \bar{\kappa}_i}.$$

Remark 2. η_i are also bounded in the sets $\Omega_{\eta i}$, i.e., $0 < \eta_i \le \bar{\eta}_i$, and $\bar{\eta}_i = \dfrac{\left(\underline{\kappa}_i + \bar{\kappa}_i\right)^2}{4\underline{\kappa}_i \bar{\kappa}_i}$, $i = 1, 2, \mathrm{K}, n$.

Proof. See Appendix A. Taking the time derivative of the state transformation function (2.5):

$$\dot{s}_i(t) = \rho_i \dot{x}_i(t) \tag{2.9}$$

where

$$\rho_i = \frac{\underline{\kappa}_i \bar{\kappa}_i \left(\underline{\kappa}_i \bar{\kappa}_i + x_i^2(t)\right)}{\left(\underline{\kappa}_i + x_i(t)\right)^2 \left(\bar{\kappa}_i - x_i(t)\right)^2}.$$

The constrained system is converted to an unconstrained system as

$$\begin{cases} \dot{s}_i = \rho_i f_i(\bar{x}_i, \ell_i) + \rho_i x_{i+1}, & i = 1, \ldots, n-1 \\ \dot{s}_n = \rho_n f_n(\bar{x}_n, \ell_n) + \rho_n g u, & u = C(v) \\ y = \eta_1 s_1 \end{cases} . \tag{2.10}$$

2.4. Error transformation

For achieving the prescribed performance and guaranteeing the transformed output tracking error to converge within the prescribed performance bounds. Firstly, we define transformed output tracking error, virtual control errors and the command filters [10] as:

$$\begin{cases} z_1 = s_1 - \alpha_{1c} \\ e_i = s_i - \alpha_{ic} \\ i = 2,3,\mathrm{K}\ ,n \end{cases}, \tag{2.11}$$

$$\begin{cases} \dot{\alpha}_{jc} = \omega \alpha_{jc,j} \\ \dot{\alpha}_{jc,j} = -2\varpi\omega\alpha_{jc,j} - \omega\left(\alpha_{jc} - \alpha_{j-1}\right), \end{cases} \tag{2.12}$$

where z_1 is the transformed output tracking error, e_i are intermediate tracking errors, α_{ic} are the outputs of the command filters, and the virtual control α_i are the inputs of the command filters. ω and $\varpi \in (0,1)$ are positive design parameters. The initial values satisfy $\alpha_{jc}(0) = \alpha_{j-1}(0)$ and $\alpha_{jc,j}(0) = 0$ for $j = 2,3,\mathrm{K}\ ,n$. α_{1c} and its time derivative are calculated as:

$$\begin{cases} \alpha_{1c} = \frac{\underline{\kappa}_1 \bar{\kappa}_1 y_r}{(\underline{\kappa}_1 + y_r)(\bar{\kappa}_1 - y_r)} \\ \dot{\alpha}_{1c} = \frac{\underline{\kappa}_1 \bar{\kappa}_1 (\underline{\kappa}_1 \bar{\kappa}_1 + y_r^2)}{(\underline{\kappa}_1 + y_r)^2 (\bar{\kappa}_1 - y_r)^2} \dot{y}_r = \rho_{1r} \dot{y}_r \end{cases} \tag{2.13}$$

where y_r is the reference signal.

To ensure the transformed output tracking error z_1 strictly converges in the prescribed performance region during the whole time, we define

$$-\underline{k}\mu(t) < z_1(t) < \bar{k}\mu(t), \quad \forall t \geq 0, \tag{2.14}$$

where the design parameters $\underline{k}$ and $\bar{k}$ are positive constants, and

$$\mu(t) = (\mu_0 - \mu_\infty) e^{-\mathrm{ht}} + \mu_\infty$$

is the prescribed performance function, $\mu(0) = \mu_0$, $0 < \mu_\infty < \mu_0$. The parameter h is also a positive constant.

Remark 3. It is obvious that the transformed output tracking error is the output tracking error of unconstrained system and is restricted in the prescribed domain, i.e. $z_1(t) \in \left(-\underline{k}\mu(t), \bar{k}\mu(t)\right)$. However, our control objective is that the output tracking error of original constrained system $e_r = x_1 - y_r$ is restricted in a prescribed domain. The output tracking error is bounded in a set

$$e_r \in \left(-\underline{k}\mu(t)\left(\underline{\kappa}_1+\bar{\kappa}_1\right)^2/\underline{\kappa}_1\bar{\kappa}_1, \bar{k}\mu(t)\left(\underline{\kappa}_1+\bar{\kappa}_1\right)^2/\underline{\kappa}_1\bar{\kappa}_1\right).$$

Proof. See Appendix B. The error transformation can be defined as:

$$z_1(t) = \mu(t)\Upsilon\left(\mathbb{Z}_1(t)\right), \forall t \geq 0 \tag{2.15}$$

where $\mathbb{Z}_1(t)$ is the transformed error and $\Upsilon(\mathbb{Z}_1)$ is defined as:

$$\Upsilon(\mathbb{Z}_1) = \frac{\bar{k}e^{\mathbb{Z}_1}-\underline{k}e^{-\mathbb{Z}_1}}{e^{\mathbb{Z}_1}+e^{-\mathbb{Z}_1}}. \tag{2.16}$$

Remark 4. It is obvious that $\Upsilon(t)$ is strictly constrained in symmetric or asymmetric domain $\left(-\underline{k}, \bar{k}\right)$ showed in Figure 3 (For the symmetric one: $\underline{k} = \bar{k} = 0.5$. For the asymmetric one: $\underline{k} = 0.5$, $\bar{k} = 0.7$). It means that the error transformation function can deal with the issues considering symmetric or asymmetric exponential constraint simultaneously.

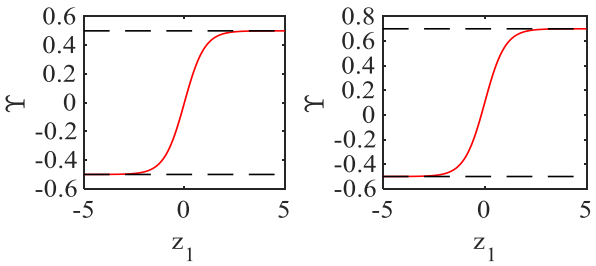

Figure 3. The relationship between z_1 and Υ (symmetric and asymmetric form).

According to (2.15) and (2.16), one can obtain:

$$\mathbb{Z}_1(t) = \Upsilon^{-1}\left(\frac{z_1(t)}{\mu(t)}\right) = \frac{1}{2}ln\frac{\Upsilon+\underline{k}}{\bar{k}-\Upsilon} \tag{2.17}$$

and

$$\dot{\mathbb{Z}}_1(t) = \rho\left(\dot{z}_1(t) - \frac{\dot{\mu}(t)z_1(t)}{\mu(t)}\right) \tag{2.18}$$

where

$$\rho = \frac{\left[\left(\frac{1}{(\Upsilon(\mathbb{Z}_1)+\underline{k})}\right)+\left(\frac{1}{(\bar{k}-\Upsilon(\mathbb{Z}_1))}\right)\right]}{2}\mu(t).$$

We finally define the transformed tracking error as

$$e_1 = \mathbb{Z}_1(t). \tag{2.19}$$

3. Controller design

In order to reduce the errors caused by the command filters, we introduce compensation signals

ς_i, and the compensation errors can be defined as $v_i = e_i - \varsigma_i$, $i = 1,\mathrm{K}\ ,n$.

FWNN is used to approximate the system uncertainties and external disturbances f_i:

$$f_i = \theta_i^T \xi_i(\mathbb{Z}) + \varepsilon_i(\mathbb{Z}). \tag{3.1}$$

For facilitating adaptive law design, we define

$$\begin{cases} \bar{\theta}_i = \max\left\{\|\theta_i\|^2, \varepsilon_{Mi}^2\right\} \\ \theta = \max\left\{\bar{\theta}_1, \mathrm{K}\ , \bar{\theta}_n\right\} \end{cases}, \quad i = 1,\mathrm{K}\ ,n, \tag{3.2}$$

where $\bar{\theta}_i$ are unknown virtual parameters with $\bar{\theta}_i < \theta$. θ_i is the ideal constant weight of ith NN and ε_{Mi} is the upper bound of approximation error ε_i.

Assumption 1. The reference trajectory y_r is continuous, and satisfies

$$[y_r, \dot{y}_r, \ddot{y}_r]^T \in \Xi_r,$$

Ξ_r is a known compact set

$$\{[y_r, \dot{y}_r, \ddot{y}_r]^T : y_d^2 + \dot{y}_d^2 + \ddot{y}_d^2 \le B_r\} \subset R^3.$$

B_r is a known positive constant. Furthermore, $-\underline{\kappa}_1 < y_r < \bar{\kappa}_1$ holds.

Assumption 2. There are some constants $\bar{\Delta}$, $\underline{g}$ and $\bar{g}$ which satisfied $\Delta(v) \le \bar{\Delta}$ and $\underline{g} \le |g| \le \bar{g}$.

For solving the unknown gain and input constraint of systems simultaneously, Nussbaum function is introduced [10]. Obviously, a Nussbaum-type function $N(\chi)$ needs to hold following the properties:

$$\begin{cases} \limsup\limits_{s\to+\infty} \dfrac{1}{s}\displaystyle\int_0^s N(\chi)\,d\chi = +\infty \\ \liminf\limits_{s\to+\infty} \dfrac{1}{s}\displaystyle\int_0^s N(\chi)\,d\chi = -\infty \end{cases}. \tag{3.3}$$

In general, $\ln(\chi+1)\cos\sqrt{\ln(\chi+1)}$, $\chi^2\cos(\chi)$ and $e^{\chi^2}\cos(\pi\chi/2)$ are commonly used Nussbaum-type function, and $N(\chi) = \chi^2\cos(\chi)$ is employed in this paper.

Lemma 2 [10]**.** Let $V(\cdot)$ and $\chi(\cdot)$ be smooth functions defined on $\left[0, t_f\right)$ with $V(t) \ge 0$. $\forall t \in \left[0, t_f\right)$, and $N(\cdot)$ is a smooth Nussbaum-type function. If the following inequality holds:

$$V(t) \le c_0 + \int_0^t \left(g_f N(\chi) + 1\right)\dot{\chi}\,d\tau \tag{3.4}$$

where g_f is a non-zero parameter and c_0 is an appropriate constant, then $V(t)$, $\chi(t)$ and $\int_0^t \left(gN(\chi)+1\right)\dot{\chi}\,d\tau$ must be bounded on $\left[0, t_f\right)$.

Step 1. Taking the time derivative of e_1 based on (2.17)–(2.19), it has:

$$\dot{e}_1 = \rho\left(\rho_1 x_2 + \rho_1 f_1 - \rho_{1r}\dot{y}_r - \frac{\dot{\mu}(t)z_1(t)}{\mu(t)}\right). \tag{3.5}$$

The error compensation signal is constructed as

$$\dot{\varsigma}_1 = -k_1\varsigma_1 + \rho\rho_1\eta_2(\varsigma_2 + \alpha_{2c} - \alpha_1). \tag{3.6}$$

Choosing a Lyapunov function and taking its time derivative, one can obtain

$$\begin{cases} V_1 = \frac{1}{2}v_1^2 + \frac{1}{2\gamma}\tilde{\theta}^2 \\ \dot{V}_1 = v_1\left(\rho\left(\rho_1\eta_2(e_2 + \alpha_{2c}) + \rho_1 f_1 - \rho_{1r}\dot{y}_r - \frac{\dot{\mu}(t)z_1(t)}{\mu(t)}\right) - \dot{\varsigma}_1\right) + \frac{1}{\gamma}\tilde{\theta}\dot{\hat{\theta}} \end{cases} \tag{3.7}$$

where the compensation error $v_1 = e_1 - \varsigma_1$.

Using a FWNN to approximate the unknown item f_1, one can obtain:

$$\dot{V}_1 = v_1\left(\rho\left(\rho_1\eta_2(e_2 + \alpha_{2c}) + \rho_1(\theta_1^T\xi_1 + \varepsilon_1) - \rho_{1r}\dot{y}_r - \frac{\dot{\mu}(t)z_1(t)}{\mu(t)}\right) - \dot{\varsigma}_1\right) + \frac{1}{\gamma}\tilde{\theta}\dot{\hat{\theta}}. \tag{3.8}$$

By the Young's inequality, it has

$$\begin{cases} \rho\rho_1 v_1\theta_1^T\xi_1 \le \rho^2\rho_1^2 v_1^2\left\|\theta_1\right\|^2\left\|\xi_1\right\|^2 + \dfrac{1}{4} \\ \rho\rho_1 v_1\varepsilon_1 \le \rho^2\rho_1^2 v_1^2\varepsilon_{M1}^2 + \dfrac{1}{4} \end{cases}. \tag{3.9}$$

Therefore, we have

$$\rho\rho_1 v_1\left(\theta_1^T\xi_1 + \varepsilon_1\right) \le \bar{\theta}_1 v_1^2\zeta_1 + \frac{1}{2} \le \theta v_1^2\zeta_1 + \frac{1}{2}, \tag{3.10}$$

with

$$\bar{\theta}_1 = \max\left\{\left\|\theta_1\right\|^2, \varepsilon_{M1}^2\right\}, \tag{3.11}$$

$$\zeta_1 = \rho^2\rho_1^2\left\|\xi_1\right\|^2 + \rho^2\rho_1^2 > 0. \tag{3.12}$$

Hence, it has

$$\dot{V}_1 \le v_1\left(\rho\left(\rho_1\eta_2(e_2 + \alpha_{2c}) - \rho_{1r}\dot{y}_r - \frac{\dot{\mu}(t)z_1(t)}{\mu(t)}\right) - \dot{\varsigma}_1\right) + \theta v_1^2\zeta_1 + \frac{1}{2} + \frac{1}{\gamma}\tilde{\theta}\dot{\hat{\theta}}. \tag{3.13}$$

By substituting compensation signal $\dot{\varsigma}_1$ from (3.6) into (3.13), it has

$$\dot{V}_1 \le v_1\left(\rho\rho_1\eta_2 v_2 - \rho\rho_{1r}\dot{y}_r - \rho\frac{\dot{\mu}(t)z_1(t)}{\mu(t)} + k_1\varsigma_1 + \rho\rho_1\eta_2\alpha_1\right) + \theta v_1^2\zeta_1 + \frac{1}{2} + \frac{1}{\gamma}\tilde{\theta}\dot{\hat{\theta}}. \tag{3.14}$$

Then, the virtual control law α_1 is designed as the following

$$\alpha_1 = \left(-k_1 e_1 - v_1 \hat{\theta} \zeta_1 + \rho \rho_{1r} \dot{y}_r + \rho \frac{\dot{\mu}(t) z_1(t)}{\mu(t)}\right) \rho^{-1} \rho_1^{-1} \eta_2^{-1}. \tag{3.15}$$

Substituting the virtual control α_1 into (3.14) results in

$$\dot{V}_1 \leq -k_1 v_1^2 + v_1 \left(\rho \rho_1 \eta_2 v_2 - v_1 \hat{\theta} \zeta_1\right) + \theta v_1^2 \zeta_1 + \frac{1}{2} + \frac{1}{\gamma} \tilde{\theta} \dot{\hat{\theta}}. \tag{3.16}$$

The adaptive law is given as

$$\dot{\hat{\theta}} = \gamma \sum_{k=1}^{n} v_k^2 \zeta_k - \sigma \hat{\theta}. \tag{3.17}$$

By integrating (3.16) and (3.17), we have

$$\dot{V}_1 \leq -k_1 v_1^2 + v_1 \rho \rho_1 \eta_2 v_2 + \frac{1}{2} + \tilde{\theta} \sum_{k=2}^{n} v_k^2 \zeta_k - \frac{\sigma}{\gamma} \tilde{\theta} \hat{\theta}. \tag{3.18}$$

Note that

$$-\frac{\sigma}{\gamma} \tilde{\theta} \hat{\theta} \leq -\frac{\sigma}{2\gamma} \tilde{\theta}^2 + \frac{\sigma}{2\gamma} \theta^2. \tag{3.19}$$

One has

$$\dot{V}_1 \leq -k_1 v_1^2 - \frac{\sigma}{2\gamma} \tilde{\theta}^2 + v_1 \rho \rho_1 \eta_2 v_2 + \tilde{\theta} \sum_{k=2}^{n} v_k^2 \zeta_k + \frac{\sigma}{2\gamma} \theta^2 + \frac{1}{2}. \tag{3.20}$$

Step 2. Taking the time derivative of e_2, it has:

$$\dot{e}_2 = \rho_2 \dot{x}_2 - \dot{\alpha}_{2c} = \rho_2 x_3 + \rho_2 f_2 - \dot{\alpha}_{2c}\,. \tag{3.21}$$

The error compensation signal is constructed as

$$\dot{\varsigma}_2 = -k_2 \varsigma_2 - \rho \rho_1 \eta_2 \varsigma_1 + \rho_2 \eta_3 (\varsigma_3 + \alpha_{3c} - \alpha_2). \tag{3.22}$$

Choosing a Lyapunov function and taking its time derivative, one can obtain

$$\begin{cases} V_2 = V_1 + \frac{1}{2} v_2^2 \\ \dot{V}_2 = \dot{V}_1 + v_2 (\rho_2 \eta_3 (e_3 + \alpha_{3c}) + \rho_2 f_2 - \dot{\alpha}_{2c} - \dot{\varsigma}_2) \end{cases} \tag{3.23}$$

where the compensation error $v_2 = e_2 - \varsigma_2$.

By integrating compensation signal $\dot{\varsigma}_2$ and (3.23), it has

$$\dot{V}_2 \leq -k_1 v_1^2 - \frac{\sigma}{2\gamma} \tilde{\theta}^2 + v_2 \begin{pmatrix} \rho_2 \eta_3 v_3 + \rho_2 f_2 + \rho \rho_1 \eta_2 e_1 \\ -\dot{\alpha}_{2c} + k_2 \varsigma_2 + \rho_2 \eta_3 \alpha_2 \end{pmatrix} + \tilde{\theta} \sum_{k=2}^{n} v_k^2 \zeta_k + \frac{\sigma}{2\gamma} \theta^2 + \frac{1}{2}. \tag{3.24}$$

Using a FWNN to approximate the unknown item f_2, one can obtain:

$$\dot{V}_2 \le -k_1 v_1^2 - \frac{\sigma}{2\gamma}\tilde{\theta}^2 + \tilde{\theta}\sum_{k=2}^{n} v_k^2\zeta_k + \frac{\sigma}{2\gamma}\theta^2 + \frac{1}{2} + v_2\begin{pmatrix}\rho_2\eta_3 v_3 + \rho_2(\theta_2^T\xi_2 + \varepsilon_2) \\ +\rho\rho_1\eta_2 e_1 - \dot{\alpha}_{2c} + k_2\varsigma_2 + \rho_2\eta_3\alpha_2\end{pmatrix}. \tag{3.25}$$

By the Young's inequality, it has

$$\begin{cases}\rho_2 v_2\theta_2^T\xi_2 \le \rho_2^2 v_2^2\|\theta_2\|^2\|\xi_2\|^2 + \frac{1}{4} \\ \rho_2 v_2\varepsilon_2 \le \rho_2^2 v_2^2\varepsilon_{M2}^2 + \frac{1}{4}\end{cases}. \tag{3.26}$$

Therefore, we have

$$\rho_2 v_2\left(\theta_2^T\xi_2 + \varepsilon_2\right) \le \bar{\theta}_2 v_2^2\zeta_2 + \frac{1}{2} \le \theta v_2^2\zeta_2 + \frac{1}{2}, \tag{3.27}$$

with

$$\bar{\theta}_2 = \max\left\{\|\theta_2\|^2, \varepsilon_{M2}^2\right\}, \tag{3.28}$$

$$\zeta_2 = \rho_2^2\|\xi_2\|^2 + \rho_2^2 > 0. \tag{3.29}$$

Hence, it has

$$\dot{V}_2 \le -k_1 v_1^2 - \frac{\sigma}{2\gamma}\tilde{\theta}^2 + \tilde{\theta}\sum_{k=2}^{n} v_k^2\zeta_k + \frac{\sigma}{2\gamma}\theta^2 + \frac{1}{2} + v_2\begin{pmatrix}\rho_2\eta_3 v_3 + \rho\rho_1\eta_2 e_1 \\ -\dot{\alpha}_{2c} + k_2\varsigma_2 + \rho_2\eta_3\alpha_2\end{pmatrix} + \theta v_2^2\zeta_2 + \frac{1}{2}. \tag{3.30}$$

Then, the virtual control law α_2 is designed as the following

$$\alpha_2 = \left(-k_2 e_2 - v_2\hat{\theta}\zeta_2 - \rho\rho_1\eta_2 e_1 + \dot{\alpha}_{2c}\right)\rho_2^{-1}\eta_3^{-1}. \tag{3.31}$$

Substituting the virtual control α_2 into (3.30) results in

$$\dot{V}_2 \le -k_1 v_1^2 - k_2 v_2^2 - \frac{\sigma}{2\gamma}\tilde{\theta}^2 + v_2\rho_2\eta_3 v_3 + \tilde{\theta}\sum_{k=3}^{n} v_k^2\zeta_k + \frac{\sigma}{2\gamma}\theta^2 + \frac{2}{2}. \tag{3.32}$$

Step i. Taking the time derivative of e_i, it has:

$$\dot{e}_i = \rho_i\dot{x}_i - \dot{\alpha}_{ic} = \rho_i x_{i+1} - \dot{\alpha}_{ic}. \tag{3.33}$$

The error compensation signal is constructed as

$$\dot{\varsigma}_i = -k_i\varsigma_i - \rho_{i-1}\eta_i\varsigma_{i-1} + \rho_i\eta_{i+1}(\varsigma_{i+1} + \alpha_{i+1c} - \alpha_i). \tag{3.34}$$

Choosing a Lyapunov function and taking its time derivative, one can obtain

$$\begin{cases} V_i = V_{i-1} + \frac{1}{2}v_i^2 \\ \dot{V}_i = \dot{V}_{i-1} + v_i(\rho_i\eta_{i+1}(e_{i+1} + \alpha_{i+1c}) + \rho_i f_i - \dot{\alpha}_{ic} - \dot{\varsigma}_i) \end{cases} \tag{3.35}$$

where the compensation error $v_i = e_i - \varsigma_i$.

By integrating compensation signal $\dot{\varsigma}_i$ and (3.35), it has

$$\begin{aligned} \dot{V}_i \le & -\sum_{k=1}^{i-1} k_k v_k^2 - \frac{\sigma}{2\gamma}\tilde{\theta}^2 + \tilde{\theta}\sum_{k=i}^{n} v_k^2\zeta_k + \frac{\sigma}{2\gamma}\theta^2 + \frac{i-1}{2} \\ & + v_i \begin{pmatrix} \rho_i\eta_{i+1}v_{i+1} + \rho_i f_i - \dot{\alpha}_{ic} \\ + k_i\varsigma_i + \rho_{i-1}\eta_i e_{i-1} + \rho_i\eta_{i+1}\alpha_i \end{pmatrix}. \end{aligned} \tag{3.36}$$

Using a FWNN to approximate the unknown item f_i, one can obtain:

$$\begin{aligned} \dot{V}_i \le & -\sum_{k=1}^{i-1} k_k v_k^2 - \frac{\sigma}{2\gamma}\tilde{\theta}^2 + \tilde{\theta}\sum_{k=i}^{n} v_k^2\zeta_k + \frac{\sigma}{2\gamma}\theta^2 + \frac{i-1}{2} \\ & + v_i \begin{pmatrix} \rho_i\eta_{i+1}v_{i+1} + \rho_i(\theta_i^T\xi_i + \varepsilon_i) \\ -\dot{\alpha}_{ic} + k_i\varsigma_i + \rho_{i-1}\eta_i e_{i-1} \\ + \rho_i\eta_{i+1}\alpha_i \end{pmatrix}. \end{aligned} \tag{3.37}$$

By the Young's inequality, it has

$$\begin{cases} \rho_i v_i\theta_i^T\xi_i \le \rho_i^2 v_i^2 \|\theta_i\|^2 \|\xi_i\|^2 + \frac{1}{4} \\ \rho_i v_i\varepsilon_i \le \rho_i^2 v_i^2 \varepsilon_{Mi}^2 + \frac{1}{4} \end{cases}. \tag{3.38}$$

Therefore, we have

$$\rho_i v_i\left(\theta_i^T\xi_i + \varepsilon_i\right) \le \bar{\theta}_i v_i^2\zeta_i + \frac{1}{2} \le \theta v_i^2\zeta_i + \frac{1}{2}, \tag{3.39}$$

with

$$\bar{\theta}_i = \max\left\{\|\theta_i\|^2, \varepsilon_{Mi}^2\right\}, \tag{3.40}$$

$$\zeta_i = \rho_i^2\|\xi_i\|^2 + \rho_i^2 > 0. \tag{3.41}$$

Hence, it has

$$\dot{V}_i \le -\sum_{k=1}^{i-1} k_k v_k^2 - \frac{\sigma}{2\gamma}\tilde{\theta}\dot{\hat{\theta}} + \tilde{\theta}\sum_{k=i}^{n} v_k^2\zeta_k + \frac{\sigma}{2\gamma}\theta^2 + \frac{i-1}{2} + v_i\begin{pmatrix}\rho_i\eta_{i+1}v_{i+1} - \dot{\alpha}_{ic} \\ +k_i\varsigma_i + \rho_{i-1}\eta_i e_{i-1} \\ +\rho_i\eta_{i+1}\alpha_i\end{pmatrix} + \theta v_i^2\zeta_i + \frac{1}{2}. \tag{3.42}$$

Then, the virtual control law α_i is designed as the following

$$\alpha_i = \left(-k_i e_i - v_i\hat{\theta}\zeta_i - \rho_{i-1}\eta_i e_{i-1} + \dot{\alpha}_{ic}\right)\rho_i^{-1}\eta_{i+1}^{-1}. \tag{3.43}$$

Substituting the virtual control α_i into (3.42) results in

$$\dot{V}_i \le -\sum_{k=1}^{i} k_k v_k^2 - \frac{\sigma}{2\gamma}\tilde{\theta}^2 + \tilde{\theta}\sum_{k=i+1}^{n} v_k^2\zeta_k + \frac{\sigma}{2\gamma}\theta^2 + \frac{i}{2} + v_i\rho_i\eta_{i+1}v_{i+1}. \tag{3.44}$$

Step n. Taking the time derivative of e_n, it has:

$$\dot{e}_n = \rho_n\dot{x}_n - \dot{\alpha}_{nc} = \rho_n g u + \rho_n f_n - \dot{\alpha}_{nc}. \tag{3.45}$$

The error compensation signal is constructed as

$$\dot{\varsigma}_n = -k_n\varsigma_n - \rho_{n-1}\eta_n\varsigma_{n-1}. \tag{3.46}$$

Choosing a Lyapunov function and taking its time derivative, one can obtain

$$\begin{cases} V_n = V_{n-1} + \frac{1}{2}v_n^2 \\ \dot{V}_n = \dot{V}_{n-1} + v_n(\rho_n g u + \rho_n f_n - \dot{\alpha}_{nc} - \dot{\varsigma}_n) \end{cases} \tag{3.47}$$

where the compensation error $v_n = e_n - \varsigma_n$.

By integrating compensation signal $\dot{\varsigma}_n$ and (3.47), it has

$$\dot{V}_n = \dot{V}_{n-1} + v_n(\rho_n g u + \rho_n f_n - \dot{\alpha}_{nc} + k_n\varsigma_n + \rho_{n-1}\eta_n\varsigma_{n-1}). \tag{3.48}$$

Using a FWNN to approximate the unknown item f_n, one can obtain:

$$\dot{V}_n = \dot{V}_{n-1} + v_n(\rho_n g u + \rho_n(\theta_n^T\xi_n + \varepsilon_n) - \dot{\alpha}_{nc} + k_n\varsigma_n + \rho_{n-1}\eta_n\varsigma_{n-1}). \tag{3.49}$$

By the Young's inequality, it has

$$\begin{cases} \rho_n v_n\theta_n^T\xi_n \le \rho_n^2 v_n^2\|\theta_n\|^2\|\xi_n\|^2 + \frac{1}{4} \\ \rho_n v_n\varepsilon_n \le \rho_n^2 v_n^2\varepsilon_{Mn}^2 + \frac{1}{4} \end{cases}. \tag{3.50}$$

Therefore, we have

$$\rho_n v_n\left(\theta_n^T\xi_n+\varepsilon_n\right)\le\bar{\theta}_n v_n^2\zeta_n+\frac{1}{2}\le\theta v_n^2\zeta_n+\frac{1}{2} \tag{3.51}$$

with

$$\bar{\theta}_n=\max\left\{\|\theta_n\|^2,\varepsilon_{Mn}^2\right\}, \tag{3.52}$$

$$\zeta_n=\rho_n^2\|\xi_n\|^2+\rho_n^2>0. \tag{3.53}$$

Hence, it has

$$\dot{V}_n\le\dot{V}_{n-1}+v_n\left(\rho_n g c_v v+\frac{1}{2}\rho_n^2 v_n-\dot{\alpha}_{nc}+k_n\varsigma_n+\rho_{n-1}\eta_n\varsigma_{n-1}\right)+\theta v_n^2\zeta_n+\frac{1}{2}+\frac{1}{2}\bar{g}^2\bar{\Delta}^2. \tag{3.54}$$

Then, the control input v is designed as the following

$$v=N(\chi)\psi\rho_n^{-1}, \tag{3.55}$$

$$\psi=k_n e_n+v_n\hat{\theta}\zeta_n+\rho_{n-1}\eta_n e_{n-1}-\dot{\alpha}_{nc}+\frac{1}{2}\rho_n^2 v_n, \tag{3.56}$$

$$\dot{\chi}=v_n\psi. \tag{3.57}$$

Substituting the virtual control v into (3.54) results in

$$\dot{V}_n\le-\sum_{k=1}^{n}k_k v_k^2+g c_v N(\chi)\dot{\chi}+\dot{\chi}-\frac{\sigma}{2\gamma}\tilde{\theta}^2+\frac{\sigma}{2\gamma}\theta^2+\frac{1}{2}\bar{g}^2\bar{\Delta}^2+\frac{n}{2}. \tag{3.58}$$

Up to now, the whole construction of LAFN-PPC is completed.

4. Stability analysis

For any given positive constant p, consider a closed set

$$\begin{cases}\Theta_1=\left\{\left(v_1,\hat{\theta}\right):v_1^2+\frac{1}{\gamma}\tilde{\theta}^2\le 2p\right\}\\ \Theta_2=\left\{\left(v_1,v_2,\hat{\theta}\right):\sum_{k=1}^{2}v_k^2+\frac{1}{\gamma}\tilde{\theta}^2\le 2p\right\}\\ \Theta_i=\left\{\left(v_1,v_2,\ldots,v_i,\hat{\theta}\right):\sum_{k=1}^{i}v_k^2+\frac{1}{\gamma}\tilde{\theta}^2\le 2p\right\}\\ \Theta_n=\left\{\left(v_1,v_2,\ldots,v_n,\hat{\theta}\right):\sum_{k=1}^{n}v_k^2+\frac{1}{\gamma}\tilde{\theta}^2\le 2p\right\}\end{cases}. \tag{4.1}$$

Theorem 1. For the strict-feedback systems (2.1) with full-state and input constraints under Assumptions 1 and 2, the controllers (3.15), (3.31), (3.43) and (3.55)–(3.57), adaptive law (3.17) and compensation signal (3.6), (3.22), (3.34) and (3.46) are constructed. If initial conditions satisfy Θ_i, $i=1,2,\mathrm{K},n$, $x_i(0)\in\left(-\underline{\kappa}_i,\bar{\kappa}_i\right)$, $i=1,2,\mathrm{K},n$, and $y_r(0)\in\left(-\underline{\kappa}_1,\bar{\kappa}_1\right)$, then the proposed control

scheme ensures the achievement of objectives (a)–(c).

Proof. The Lyapunov function choosing as

$$V = \frac{1}{2}\sum_{k=1}^{n} v_k^2 + \frac{1}{2\gamma}\tilde{\theta}^2 . \tag{4.2}$$

From (3.58), we have

$$\dot{V} \le -\sum_{k=1}^{n} k_k v_k^2 + gc_v N(\chi)\dot{\chi} + \dot{\chi} - \frac{\sigma}{2\gamma}\tilde{\theta}^2 + \frac{\sigma}{2\gamma}\theta^2 + \frac{1}{2}\bar{g}^2\bar{\Delta}^2 + \frac{n}{2} . \tag{4.3}$$

To facilitate analysis, the above inequality can be written as

$$\dot{V} \le -AV + B + (gc_v N(\chi) + 1)\dot{\chi} , \tag{4.4}$$

where

$$\mathrm{A} \le \min\{2k_1, \mathrm{K}, 2k_n, \sigma\},$$

$$\mathrm{B} = \frac{\sigma}{2\gamma}\theta^2 + \frac{1}{2}\bar{g}^2\bar{\Delta}^2 + \frac{n}{2}.$$

By computing the integration of the above differentiation inequality at the interval $[0,t)$, one can obtain

$$0 \le V \le V(0)e^{-At} + \frac{B}{A}(1 - e^{-At}) + e^{-At}\int_0^t (gc_v N(\chi) + 1)\dot{\chi}e^{A\tau}d\tau . \tag{4.5}$$

From Lemma 2, we can get that V, χ and $\int_0^t (gc_v N(\chi) + 1)\dot{\chi}d\tau$ are bounded at the interval $[0,t)$. And the result holds even if $t \to \infty$. Furthermore, let $\mathbb{C}$ be the upper bound of $e^{-At}\int_0^t (gc_v N(\chi) + 1)\dot{\chi}e^{A\tau}d\tau$. The following inequality will holds

$$V \le \left(V(0) - \frac{B}{A}\right)e^{-At} + \frac{B}{A} + \mathbb{C} . \tag{4.6}$$

We denote F_∞ as the set of all bounded functions. According to the above analysis, we can get $V \le p$. Therefore, we can obtain that v_1, v_2,⊥, v_n, θ, ς_1, ς_2,⊥, ς_n are bounded. Furthermore, e_i are also bounded due to $v_i = e_i - \varsigma_i$. As $e_1 = \mathbb{Z}_1(t)$ and $e_1 \in F_\infty$ it has $\mathbb{Z}_1(t) \in F_\infty$. It implies $z_1(t), \rho \in F_\infty$ and $s_1 = z_1 + \alpha_{1c} \in F_\infty$. Noting (2.9), we obtain $\rho_1 \in F_\infty$. From (2.18), it yields $\rho, \mu_1(t)$, $\dot{\mu}_1(t) \in F_\infty$. With the help of (3.15) and (2.12), we have $\alpha_1 \in F_\infty$ and $\alpha_{2c}, \dot{\alpha}_{2c} \in F_\infty$. Since $s_2 = v_2 + \alpha_{2c} + \varsigma_2$, we get $s_2 \in F_\infty$. Noting (2.9), we obtain $\rho_2 \in F_\infty$. From (3.31) and (2.12), we get $\alpha_2 \in F_\infty$ and $\alpha_{3c}, \dot{\alpha}_{3c} \in F_\infty$. Similarly, we can easily get

$$s_3,\ \rho_3,\ \alpha_{4c},\ \dot{\alpha}_{4c}, \cdots,\ s_{n-1},\ \rho_{n-1},\ \alpha_{nc},\ \dot{\alpha}_{nc},\ s_n,\ \rho_n,\ v \in F_\infty.$$

From (2.8), it yields $x_1,\ x_2, \cdots,\ x_n \in F_\infty$. This finishes the proof.

Remark 5. In the proposed low-cost adaptive neural prescribed performance control (LAFN-PPC) scheme, we can obtain a satisfactory performance by reasonably adjusting k_i, γ, σ, $\bar{\kappa}_i$, $\underline{\kappa}_i$, $\bar{k}$, $\underline{k}$, μ_0, μ_∞ and h, where $i=1,2,\mathrm{K},n$. The larger k_i and smaller γ, σ can improve the convergence speed and tracking accuracy of the controller. But too large k_i and small γ, σ values can result in large control input, which may be far beyond physical limitations of actuator. The adaptive parameters γ and σ play the part of regulators between controller and control output. To avoid the large control input, the values of the parameters k_i, γ, σ, $i=1,2,\mathrm{K},n$ are limited to a certain interval. Meanwhile, $\bar{\kappa}_i$ and $\underline{\kappa}_i$ are used to constrain the states $x_i(t)$ within the open sets $\left(-\underline{\kappa}_i,\bar{\kappa}_i\right)$, which can be selected according to the actual application requirements. From this it can be concluded that the time varying parameter

$$\rho_i=\left(\underline{\kappa}_i\bar{\kappa}_i\left(\underline{\kappa}_i\bar{\kappa}_i+x_i^2(t)\right)\right)\Big/\left(\left(\underline{\kappa}_i+x_i(t)\right)^2\left(\bar{\kappa}_i-x_i(t)\right)^2\right).$$

The parameters $\bar{k}$, $\underline{k}$, μ_0, μ_∞ and h are designed to constrain the transformed output tracking error within the open set $\left(-\underline{k}\mu(t),\bar{k}\mu(t)\right)$, where

$$\mu(t)=\left(\mu_0-\mu_\infty\right)e^{-\mathrm{h}t}+\mu_\infty.$$

μ_0, h and μ_∞ determine the initial error, the error convergence rate and the steady-state error of the transformed output tracking error bound, which can be selected according to the performance requirements. $\bar{k}$ and $\underline{k}$ are always within $(0,1]$ and can deal with the issues considering symmetric or asymmetric transformed output tracking error constraint.

5. Simulations

In order to prove the effectiveness and feasibility of our control scheme, this section provides comparison simulation cases. Meanwhile, the control schemes based on works in [29,30] are compared with our suggested control scheme.

A rigid manipulator system [30] is given as

$$\begin{cases} J_L\ddot{\theta}+Mg_vL\sin\theta+T_E=u \\ u=H(v) \end{cases} \tag{5.1}$$

where θ, $\dot{\theta}$ and $\ddot{\theta}$ are the position, velocity and acceleration of the link, respectively. M, g_v and L denote the link mass, gravity constant and the distance from the joint to the mass center of the link, respectively. T_E indicates the unknown external load. u is the actual control torque which is subjected to the unknown input constraint nonlinearity $H(v)$, and v is system control input signal.

To facilitate the controller design, we transfer the system (5.1) with new variables. Let $x_1=\theta$, $x_2=\dot{\theta}$. Then the dynamic model of system (5.1) can be expressed as follows:

$$\begin{cases} \dot{x}_1 = x_2 \\ \dot{x}_2 = J_L^{-1}(u - MgL\sin x_1 - T_E) \\ u = H(v) \\ y = x_1 \end{cases}. \tag{5.2}$$

To simplify the expression, the dynamic model is rewritten as

$$\begin{cases} \dot{x}_1 = x_2 \\ \dot{x}_2 = G_L u + f_L \\ u = H(v) = c_v v + \Delta(v) \\ y = x_1 \end{cases} \tag{5.3}$$

where

$$f_L = \frac{-MgL\sin x_1 - T_E}{J_L},\ G_L = J_L^{-1}.$$

In the simulation, we set $f_1(x_1) = 0$, $f_2(x_1, x_2) = f_L$ and $g = G_L$. $M = 0.35\ Kg$, g_v=9.8 m/s^2, $L = 1.47\ m$ and $T_E = 0.1\sin t$. The tracking signal of following cases are set as $y_r = 0.5\sin t$.

Case 1. The initial system states and output are $x(0) = [0.1, 0]$. And $\hat{\theta}(0) = \alpha_{jc}(0) = \alpha_{jc,j}(0) = 0$, $\varsigma_1(0) = \varsigma_2(0) = 0$. The proposed controller, adaptive laws and error compensation schemes are constructed as

$$\begin{cases} \alpha_1 = \left(-k_1 e_1 + \rho\rho_{1r}\dot{y}_r + \rho\frac{\dot{\mu}(t)z_1(t)}{\mu(t)}\right)\rho^{-1}\rho_1^{-1}\eta_2^{-1} \\ v = N(\chi)\psi\rho_2^{-1} \\ \psi = k_2 e_2 + v_2\hat{\theta}\zeta + \rho\rho_1\eta_2 e_1 - \dot{\alpha}_{nc} + \frac{1}{2}\rho_2^2 v_2 \\ \dot{\chi} = v_2\psi \end{cases}, \tag{5.4}$$

$$\begin{cases} \dot{\varsigma}_1 = -k_1\varsigma_1 + \rho\rho_1\eta_2(\varsigma_2 + \alpha_{2c} - \alpha_1) \\ \dot{\varsigma}_2 = -k_2\varsigma_2 - \rho\rho_1\eta_2\varsigma_1 \end{cases}, \tag{5.5}$$

$$\dot{\hat{\theta}} = \gamma v_2^2\zeta_2 - \sigma\hat{\theta}, \tag{5.6}$$

where the parameters are chosen as $k_1 = 50$, $k_2 = 15$, $\gamma = 10$, $\sigma = 0.7$, $\omega = 300$, $\varpi = 0.95$. The parameters of FWNN are chosen as: The nodes of neural network is 7, the center c_1^j is distributed in the field of $[-3, 3]$, and its width $\omega_1^j = 1$. The parameters of full-state constraints, input constraint and prescribed performance constraint are set as: $\bar{\kappa}_1 = 1.5$, $\underline{\kappa}_1 = 1.5$, $\underline{\kappa}_2 = 3$, $\bar{\kappa}_2 = 4$, $u^+ = 30$, $u^- = -30$, $\mu_0 = 0.2$, $\mu_\infty = 0.02$, h = 1, $\underline{k} = 1$, $\bar{k} = 1$.

Case 2. Base on the case 1, we further study the output tracking errors when give different prescribed performance. e_{r1} for $\mu_\infty = 0.02$, e_{r2} for $\mu_\infty = 0.016$, e_{r3} for $\mu_\infty = 0.012$, e_{r4} for $\mu_\infty = 0.008$, e_{r5} for $\mu_\infty = 0.004$, e_{r6} for $\mu_\infty = 0.002$.

Case 3. Based on the case 2, we set $\mu_\infty = 0.004$ and $y_d = y_r$, two comparative simulation from [29,30] are carried out to further show the advantage of our control scheme, which is still based on the rigid

manipulator system (5.3). The controller, adaptive laws and first-order filter of work in [29] are given as

$$\begin{cases} \alpha_1 = -c_1 \frac{\underline{F}_1\bar{F}_1\left(\underline{F}_1\bar{F}_1 - x_1^2\right)}{\left(\underline{F}_1 + x_1\right)^2\left(\bar{F}_1 - x_1\right)^2} z_1 + \frac{\underline{F}_1\bar{F}_1\left(\underline{F}_1\bar{F}_1 - y_d^2\right)}{\left(\underline{F}_1 + y_d\right)^2\left(\bar{F}_1 - y_d\right)^2}\dot{y}_d \\ u = -\left(c_2 + \hat{\theta}\Phi\right)\frac{\underline{F}_2\bar{F}_2\left(\underline{F}_2\bar{F}_2 - x_2^2\right)}{\left(\underline{F}_2 + x_2\right)^2\left(\bar{F}_2 - x_2\right)^2} z_2 \\ \Phi = \left\| \frac{\underline{F}_1\bar{F}_1\left(\underline{F}_1\bar{F}_1 - x_1^2\right)}{\left(\underline{F}_1 + x_1\right)^2\left(\bar{F}_1 - x_1\right)^2} \right\|^2 \left(1 + \varphi^2\right) + \left\|\dot{\alpha}_{2f}\right\|^2 \end{cases}, \tag{5.7}$$

$$\dot{\hat{\theta}} = \gamma \|z_2\|^2 \Phi - \sigma\widehat{\theta}, \tag{5.8}$$

$$\varepsilon\dot{\alpha}_{2f} + \alpha_{2f} = \frac{\underline{F}_2\bar{F}_2}{\left(\underline{F}_2 + x_2\right)\left(\bar{F}_2 - x_2\right)}\alpha_1, \tag{5.9}$$

where $z_1 = x_1 - y_d$, $z_2 = x_2 - \alpha_{2f}$, $\theta(0) = 0$, $\alpha_{2f}(0) = 0$, $c_1 = 40$, $c_2 = 80$, $\underline{F}_1 = 1.5$, $\bar{F}_1 = 1.5$, $\underline{F}_2 = 3$, $\bar{F}_2 = 4$, $\gamma = 15$, $\sigma = 0.5$, $\varphi = 5$ and $\varepsilon = 0.03$. Detailed controller design and parameter meaning is found in [29].

The controller, adaptive laws and first-order filter of works in [30]. are given as

$$\begin{cases} \alpha_1 = -\left(\frac{\underline{k}_1\bar{k}_1\left(\underline{k}_1\bar{k}_1 + x_1^2\right)}{\left(\underline{k}_1 + x_1\right)^2\left(\bar{k}_1 - x_1\right)^2}\right)^{-1}\left(k_1 z_1 - \frac{\underline{k}_1\bar{k}_1\left(\underline{k}_1\bar{k}_1 + y_d^2\right)}{\left(\underline{k}_1 + y_d\right)^2\left(\bar{k}_1 - y_d\right)^2}\dot{y}_d\right) \\ \mu = N(\zeta_2)v_2 \\ v_2 = \left(\frac{\underline{k}_2\bar{k}_2\left(\underline{k}_2\bar{k}_2 + x_2^2\right)}{\left(\underline{k}_2 + x_2\right)^2\left(\bar{k}_2 - x_2\right)^2}\right)^{-1}\left(k_2 z_2 + z_2\hat{\theta}^T\phi(Z) - \dot{\psi}_2\right) \\ \dot{\zeta}_2 = \frac{\underline{k}_2\bar{k}_2\left(\underline{k}_2\bar{k}_2 + x_2^2\right)}{\left(\underline{k}_2 + x_2\right)^2\left(\bar{k}_2 - x_2\right)^2} z_2 v_2 \end{cases}, \tag{5.10}$$

$$\dot{\hat{\theta}} = \Gamma\left(\phi(Z)z_2^2 - \sigma\hat{\theta}\right), \tag{5.11}$$

$$\delta\dot{\psi}_2 + \psi_2 = \frac{\underline{k}_2\bar{k}_2}{\left(\underline{k}_2 + x_2\right)\left(\bar{k}_2 - x_2\right)}\alpha_1, \tag{5.12}$$

where $z_1 = x_1 - y_d$, $z_2 = x_2 - \psi_2$, $\zeta_2(0) = 0$, $\psi_2(0) = 0$, $k_1 = 50$, $k_2 = 30$, $\underline{k}_1 = 1.5$, $\bar{k}_1 = 1.5$, $\underline{k}_2 = 3$, $\bar{k}_2 = 4$, $\Gamma = 15$ and $\sigma = 0.5$. $\phi(Z)$ is the activation function of neural network, Z is the input of neural network. The parameters of RBF are chosen as: The nodes of neural network is 7, the center μ_1 is distributed in the field of $[-0.3, 0.3]$, and its width $\sigma_1 = 0.1$. Detailed controller design and parameter meaning is found in [30].

Figures 4–7 reflect the main results of our control scheme. Figure 4 shows that output y of rigid manipulator system can track desired trajectory well without violating the output constraint. Figure 5 reveals the output tracking error e_r is in the region boundary all the times. The actual controls u is showed in Figure 6. And the state x_2 is illustrated in Figure 7. From Figure 8, the proposed control scheme tracks the desired signal well with different prescribed performance, and the boundedness of prescribed performance is not violated.

Figures 9–11 present the comparative results of tracking trajectories, output tracking errors and input signals. We can easily find that the results of LAFN-PPC is better than controllers in [29,30]. Hence, for strict-feedback systems with purpose of high-precision tracking performance, full-state constraints and input constraint, we can conclude that our suggested control scheme has a potential to control them.

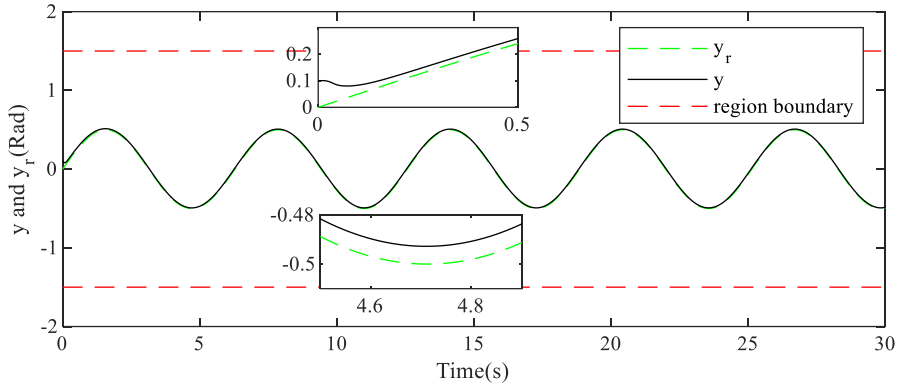

Figure 4. Output tracking.

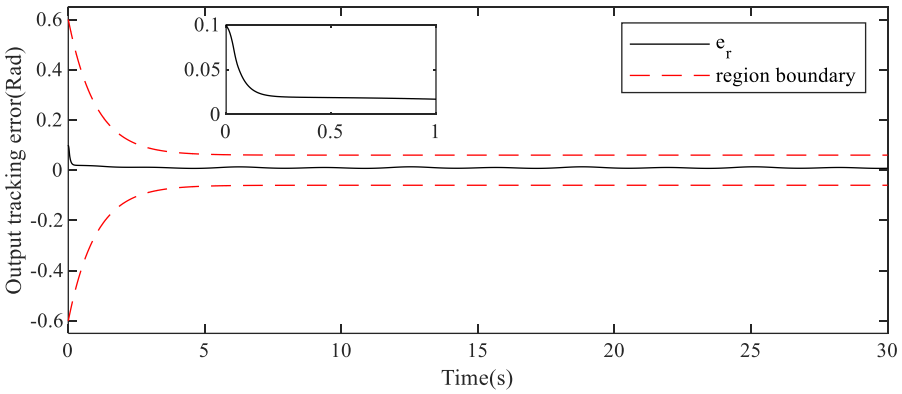

Figure 5. Output tracking error.

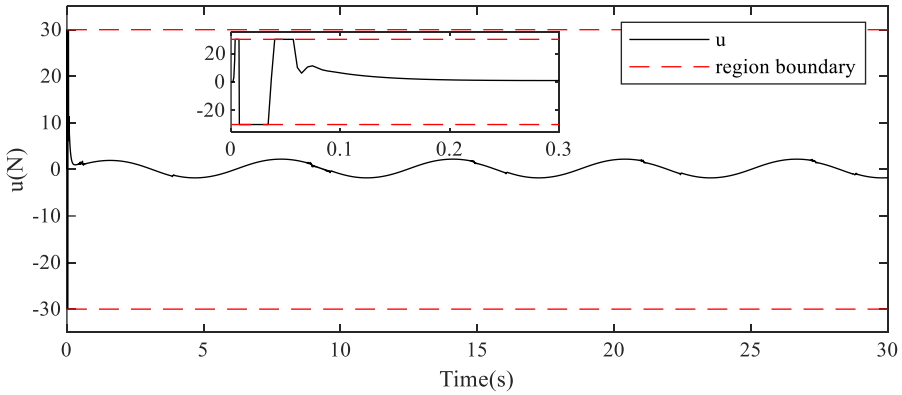

Figure 6. Trajectory of actual control u.

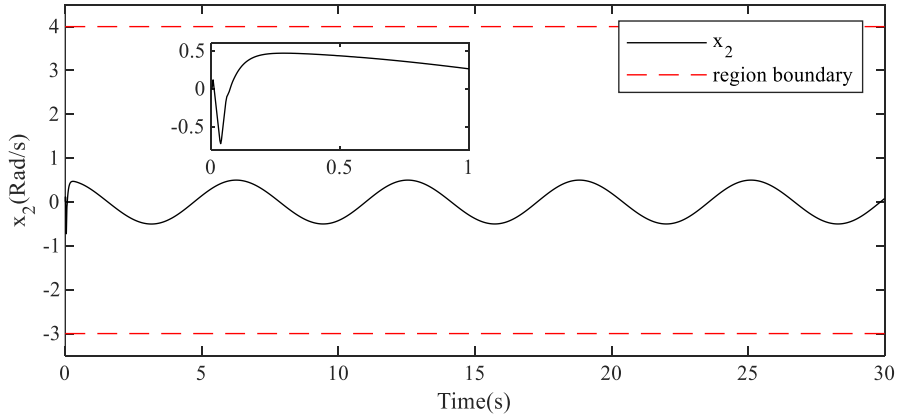

Figure 7. Response of system state x_2.

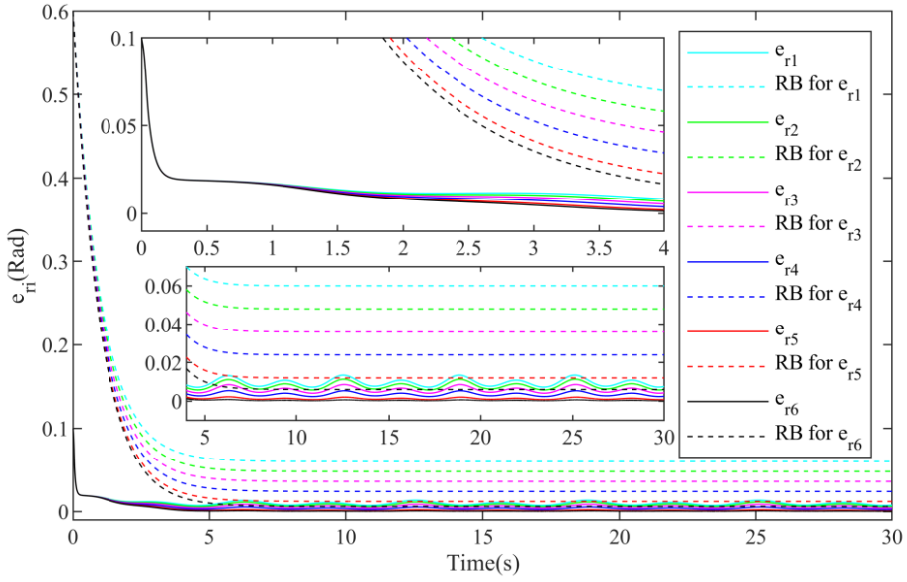

Figure 8. Output tracking errors for different prescribed performance.

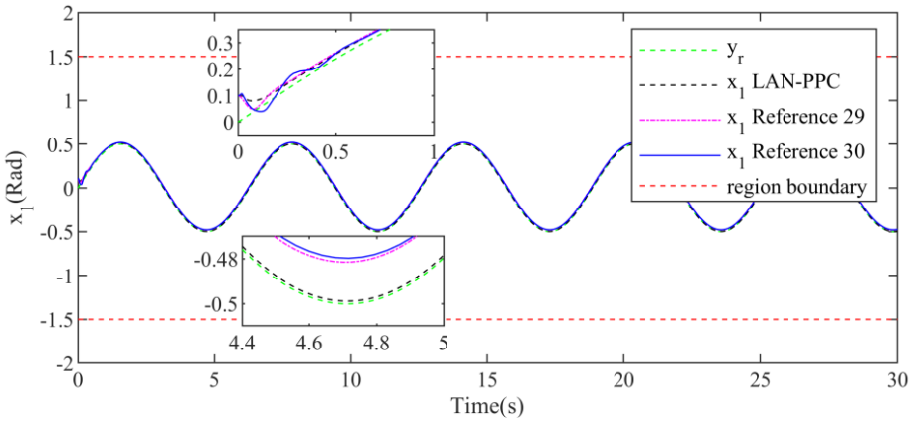

Figure 9. Comparison of output tracking with works in [29,30].

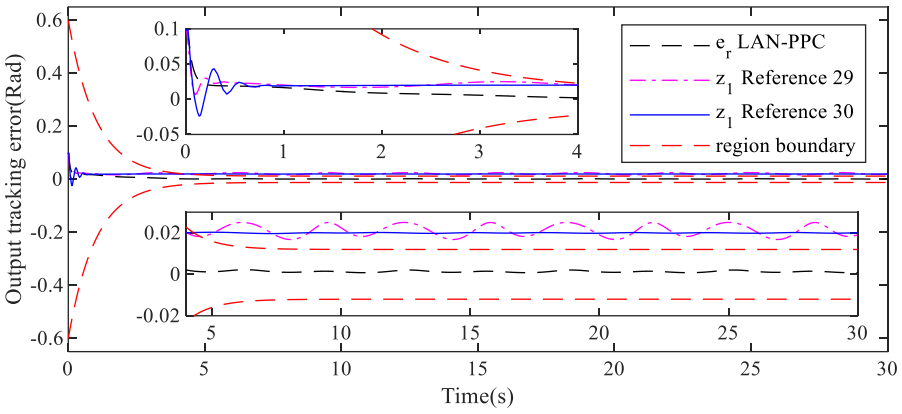

Figure 10. Comparison of output tracking error with works in [29,30].

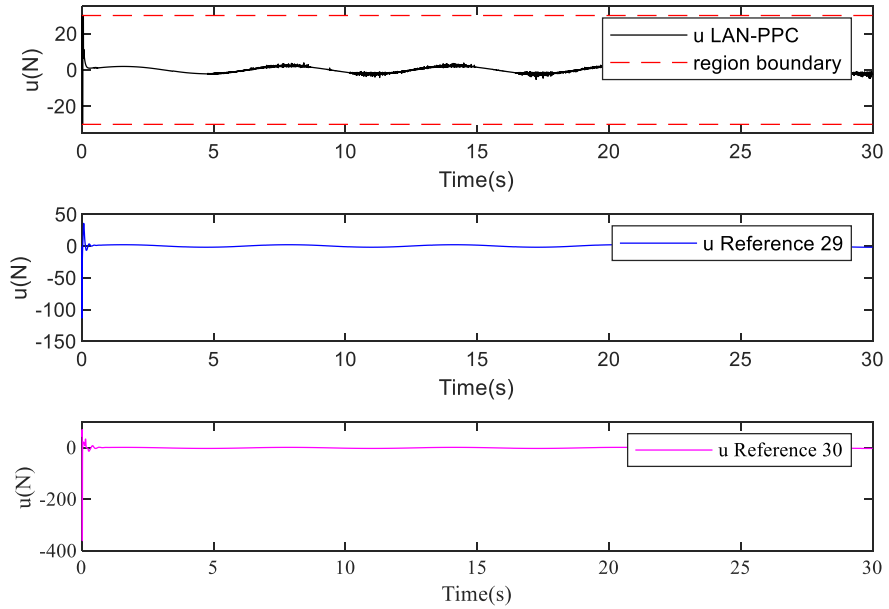

Figure 11. Comparison of input signal with works in [29,30].

6. Conclusions

The LAFN-PPC is newly constructed for strict-feedback systems with prescribed output performance, full-state constraints and input constraint. The newly constructed command filter based adaptive control scheme with an error compensation mechanism can not only overcome the so-called "EOC" problem, but also reduce filter errors. By introducing a one-to-one nonlinear state transformation function, the full-state constraints are resolved. The prescribed performance can be guaranteed by using the one-to-one nonlinear error transformation function. The unknown control direction and the input constraint nonlinearity are resolved by introducing the Nussbaum function simultaneously. Moreover, the large computational cost is solved by introducing a virtual parameter of adaptive laws. Only one parameter needs to be updated online. Future works can focus on command-filter based optimal control of nonstrict-feedback systems considering performance constraint and address how to minimize resources consumption while ensuring performance.

Appendix A.

Proof. According to the state transformation function (2.8), we have

$$\eta_i = \frac{-x_i^2 + \left(\bar{\kappa}_i - \underline{\kappa}_i\right) x_i + \underline{\kappa}_i \bar{\kappa}_i}{\underline{\kappa}_i \bar{\kappa}_i}. \tag{A.1}$$

x_i are always constrained in the open sets $\left(-\underline{\kappa}_i, \bar{\kappa}_i\right)$, i.e., $x_i(t) \in \Omega_i$. Therefore, we can easily obtain that $\eta_i > 0$ and η_i take the maximal value at the points $x_i^0 = \left(\bar{\kappa}_i - \underline{\kappa}_i\right)/2$ according to the properties of the quadratic function. It is obvious that x_i^0 is in the interval $\left(-\underline{\kappa}_i, \bar{\kappa}_i\right)$. Thus, the maximal value of η_i is

$$\bar{\eta}_i = \frac{\left(\bar{\kappa}_i + \underline{\kappa}_i\right)^2}{4\underline{\kappa}_i \bar{\kappa}_i}, \quad i = 1, 2, \mathrm{L}\ , n. \tag{A.2}$$

This finishes the proof.

Appendix B.

Proof. According to (2.5), (2.11), (2.13) and (2.14), we have

$$\begin{aligned}
s_1 - \alpha_{1c} &= \frac{\underline{\kappa}_1 \bar{\kappa}_1 x_1}{\left(\underline{\kappa}_1 + x_1\right)\left(\bar{\kappa}_1 - x_1\right)} - \frac{\underline{\kappa}_1 \bar{\kappa}_1 y_r}{\left(\underline{\kappa}_1 + y_r\right)\left(\bar{\kappa}_1 - y_r\right)} \\
&= \left(-\frac{\underline{\kappa}_1^2 \bar{\kappa}_1}{\underline{\kappa}_1 + \bar{\kappa}_1} \frac{1}{\underline{\kappa}_1 + x_1} + \frac{\underline{\kappa}_1 \bar{\kappa}_1^2}{\underline{\kappa}_1 + \bar{\kappa}_1} \frac{1}{\bar{\kappa}_1 - x_1} \right) - \left(-\frac{\underline{\kappa}_1^2 \bar{\kappa}_1}{\underline{\kappa}_1 + \bar{\kappa}_1} \frac{1}{\underline{\kappa}_1 + y_r} + \frac{\underline{\kappa}_1 \bar{\kappa}_1^2}{\underline{\kappa}_1 + \bar{\kappa}_1} \frac{1}{\bar{\kappa}_1 - y_r} \right) \\
&= \frac{\underline{\kappa}_1^2 \bar{\kappa}_1}{\underline{\kappa}_1 + \bar{\kappa}_1} \left(\frac{1}{\underline{\kappa}_1 + y_r} - \frac{1}{\underline{\kappa}_1 + x_1} \right) + \frac{\underline{\kappa}_1 \bar{\kappa}_1^2}{\underline{\kappa}_1 + \bar{\kappa}_1} \left(\frac{1}{\bar{\kappa}_1 - x_1} - \frac{1}{\bar{\kappa}_1 - y_r} \right) \\
&= \frac{\underline{\kappa}_1^2 \bar{\kappa}_1}{\underline{\kappa}_1 + \bar{\kappa}_1} \frac{x_1 - y_r}{\left(\underline{\kappa}_1 + y_r\right)\left(\underline{\kappa}_1 + x_1\right)} + \frac{\underline{\kappa}_1 \bar{\kappa}_1^2}{\underline{\kappa}_1 + \bar{\kappa}_1} \frac{x_1 - y_r}{\left(\bar{\kappa}_1 - x_1\right)\left(\bar{\kappa}_1 - y_r\right)} \\
&= \left[\frac{\underline{\kappa}_1^2 \bar{\kappa}_1}{\left(\underline{\kappa}_1 + \bar{\kappa}_1\right)\left(\underline{\kappa}_1 + y_r\right)\left(\underline{\kappa}_1 + x_1\right)} + \frac{\underline{\kappa}_1 \bar{\kappa}_1^2}{\left(\underline{\kappa}_1 + \bar{\kappa}_1\right)\left(\bar{\kappa}_1 - x_1\right)\left(\bar{\kappa}_1 - y_r\right)} \right] \left(x_1 - y_r\right)
\end{aligned}. \tag{B.1}$$

x_1 and y_r are constrained in the open sets $\left(-\underline{\kappa}_i, \bar{\kappa}_i\right)$. Thus, $0 < \underline{\kappa}_1 + y_r < \underline{\kappa}_1 + \bar{\kappa}_1$, $0 < \underline{\kappa}_1 + x_1 < \underline{\kappa}_1 + \bar{\kappa}_1$, $0 < \bar{\kappa}_1 - x_1 < \underline{\kappa}_1 + \bar{\kappa}_1$ and $0 < \bar{\kappa}_1 - y_r < \underline{\kappa}_1 + \bar{\kappa}_1$. One obtains

$$\begin{aligned}
0 &< \frac{\underline{\kappa}_1^2 \bar{\kappa}_1}{\left(\underline{\kappa}_1 + \bar{\kappa}_1\right)\left(\underline{\kappa}_1 + y_r\right)\left(\underline{\kappa}_1 + x_1\right)} + \frac{\underline{\kappa}_1 \bar{\kappa}_1^2}{\left(\underline{\kappa}_1 + \bar{\kappa}_1\right)\left(\bar{\kappa}_1 - x_1\right)\left(\bar{\kappa}_1 - y_r\right)} \\
&< \frac{\underline{\kappa}_1^2 \bar{\kappa}_1}{\left(\underline{\kappa}_1 + \bar{\kappa}_1\right)^3} + \frac{\underline{\kappa}_1 \bar{\kappa}_1^2}{\left(\underline{\kappa}_1 + \bar{\kappa}_1\right)^3} = \frac{\underline{\kappa}_1 \bar{\kappa}_1}{\left(\underline{\kappa}_1 + \bar{\kappa}_1\right)^2}
\end{aligned}. \tag{B.2}$$

The transformed output tracking error $z_1 = s_1 - \alpha_{1c}$ strictly converges in the prescribed performance region $-\underline{k}\mu(t) < z_1(t) < \bar{k}\mu(t)$. Hence, it has

$$-\frac{\underline{k}\mu(t)\left(\underline{\kappa}_1 + \bar{\kappa}_1\right)^2}{\underline{\kappa}_1\bar{\kappa}_1} < x_1 - y_r < \frac{\bar{k}\mu(t)\left(\underline{\kappa}_1 + \bar{\kappa}_1\right)^2}{\underline{\kappa}_1\bar{\kappa}_1}. \tag{B.3}$$

This finishes the proof.

Acknowledgments

The authors would like to appreciate all the editors and reviewers for improving the quality of this article. This work was supported by the National Key Research and Development Program of China (2018YFB1304800) and Key Research and Development Program of Guangdong Province (2020B090926002).

Conflict of interest

All authors declare no conflicts of interest in this paper.

References

1. C. M. Kwan, F. L. Lewis, Robust backstepping control of induction motors using neural networks, *IEEE T. Neur. Net.*, **11** (2000), 1178–1187. https://doi.org/10.1109/72.870049
2. Q. Zhou, S. Y. Zhao, H. Y. Li, R. Q. Lu, C. W. Wu, Adaptive neural network tracking control for robotic manipulators with dead zone, *IEEE T. Neur. Net.*, **30** (2019), 3611–3620. https://doi.org/10.1109/TNNLS.2018.2869375
3. S. H. Luo, F. L. Lewis, Y. D. Song, R. Garrappa, Dynamical analysis and accelerated optimal stabilization of the fractional-order self-sustained electromechanical seismograph system with fuzzy wavelet neural network, *Nonlinear Dyn.*, **104** (2021), 1389–1404. https://doi.org/10.1007/s11071-021-06330-5
4. S. G. Gao, H. R. Dong, B. Ning, X. B. Sun, Neural adaptive control for uncertain MIMO systems with constrained input via intercepted adaptation and single learning parameter approach, *Nonlinear Dyn.*, **82** (2015), 1109–1126. https://doi.org/10.1007/s11071-015-2220-0
5. S. H. Luo, F. L. Lewis, Y. D. Song, H. M. Ouakad, Optimal synchronization of unidirectionally coupled FO chaotic electromechanical devices with the hierarchical neural network, unpublished work.
6. Y. X. Li, G. H. Yang, Event-triggered adaptive backstepping control for parametric strict-feedback nonlinear systems, *Int. J. Robust Nonlinear Contr.*, **28** (2018), 976–1000. https://doi.org/10.1002/rnc.3914
7. H. Ma, H. J. Liang, H. J. Ma, Q. Zhou, Nussbaum gain adaptive backstepping control of nonlinear strict-feedback systems with unmodeled dynamics and unknown dead zone, *Int. J. Robust Nonlinear Control*, **28** (2018), 5326–5343. https://doi.org/10.1002/rnc.4315
8. C. L. Wang, Y. Lin, Multivariable adaptive backstepping control: A norm estimation approach, *IEEE T. Automatic Contr.*, **57** (2012), 989–995. https://doi.org/10.1109/TAC.2011.2167815

9. D. Swaroop, J. K. Hedrick, P. P. Yip, J. C. Gerdes, Dynamic surface control for a class of nonlinear systems, *IEEE T. Automatic Contr.*, **45** (2000), 1893–1899. https://doi.org/10.1109/TAC.2000.880994
10. S. S. Ge, J. Wang, Robust adaptive tracking for time-varying uncertain nonlinear systems with unknown control coefficients, *IEEE T. Automatic Contr.*, **48** (2003), 1463–1469. https://doi.org/10.1109/TAC.2003.815049
11. H. Wang, Q. P. Shi, H. Y. Li, Q. Zhou, Adaptive neural tracking control for a class of nonlinear systems with dynamic uncertainties, *IEEE T. Cybernetics*, **47** (2017), 3075–3087. https://doi.org/10.1109/TCYB.2016.2607166
12. Q. Zhou, L. J. Wang, C. W. Wu, H. Y. Li, Adaptive fuzzy tracking control for a class of pure-feedback nonlinear systems with time-varying delay and unknown dead zone, *Fuzzy Sets Syst.*, **329** (2017), 36–60. https://doi.org/10.1016/j.fss.2016.11.005
13. W. He, T. T. Meng, X. Y. He, C. Y. Sun, Iterative learning control for a flapping wing micro aerial vehicle under distributed disturbances, *IEEE T. Cybernetics*, **49** (2019), 1524–1535. https://doi.org/10.1109/TCYB.2018.2808321
14. M. Krstic, I. Kanellakopoulos, P. V. Kokotovic, Adaptive nonlinear control without overparametrization, *Syst. Control Lett.*, **19** (1992), 177–185. https://doi.org/10.1016/0167-6911(92)90111-5
15. M. Krstic, I. Kanellakopoulos, P. V. Kokotovic, *Nonlinear and adaptive control design*, Wiley, 1995.
16. C. Chen, C. Y. Wen, Z. Liu, K. Xie, Y. Zhang, C. L. P. Chen, Adaptive asymptotic control of multivariable systems based on a one-parameter estimation approach, *Automatica*, **83** (2017), 124–132. https://doi.org/10.1016/j.automatica.2017.03.003
17. K. Zhao, Y. D. Song, W. C. Meng, C. L. P. Chen, L. Chen, Low-cost approximation-based adaptive tracking control of output-constrained nonlinear systems, *IEEE T. Neur. Net. Lear. Syst.*, **32** (2021), 4890–4900. https://doi.org/10.1109/TNNLS.2020.3026078
18. L. Zhao, S. H. Luo, G. C. Yang, R. Z. Dong, Chaos analysis and stability control of the MEMS resonator via the type-2 sequential FNN, *Microsyst. Technol.*, **21** (2020), 173–182. https://doi.org/10.1007/s00542-020-04935-1
19. S. B. Yang, X. Wang, H. N. Wang, Y. G. Li, Sliding mode control with system constraints for aircraft engines, *ISA T.*, **98** (2020), 1–10. https://doi.org/10.1016/j.isatra.2019.08.020
20. S. H. Luo, F. L. Lewis, Y. D. Song, K. G. Vamvoudakis, Adaptive backstepping optimal control of a fractional-order chaotic magnetic-field electromechanical transducer, *Nonlinear Dyn.*, **100** (2020), 523–540. https://doi.org/10.1007/s11071-020-05518-5
21. H. Y. Li, L. Bai, Q. Zhou, R. Q. Lu, L. J. Wang, Adaptive fuzzy control of stochastic nonstrict-feedback nonlinear systems with input saturation, *IEEE T. Syst. Man Cybernetics*, **47** (2017), 2185–2188. https://doi.org/10.1109/TSMC.2016.2635678
22. R. B. Li, B. Niu, Z. G. Feng, J. Q. Li, P. Y. Duan, D. Yang, Adaptive neural design frame for uncertain stochastic nonlinear non-lower triangular pure-feedback systems with input constraint, *J. Franklin Inst.*, **356** (2019), 9545–9564. https://doi.org/10.1016/j.jfranklin.2019.09.019
23. W. J. Si, X. D. Dong, F. F. Yang, Decentralized adaptive neural control for interconnected stochastic nonlinear delay-time systems with asymmetric saturation actuators and output constraints, *J. Franklin Inst.*, **355** (2018), 54–80. https://doi.org/10.1016/j.jfranklin.2017.11.002

24. B. Xu, F. C. Sun, C. G. Yang, D. X. Gao, J. X. Ren, Adaptive discrete-time controller design with neural network for hypersonic flight vehicle via back-stepping, *Int. J. Control*, **84** (2011), 1543–1552. https://doi.org/10.1080/00207179.2011.615866
25. J. X. Zhang, S. L. Wang, P. Zhou, L. Zhao, S. B. Li, Novel prescribed performance-tangent barrier Lyapunov function for neural adaptive control of the chaotic PMSM system by backstepping, *Int. J. Elec. Power Energy Syst.*, **121** (2020), 105991. https://doi.org/10.1016/j.ijepes.2020.105991
26. K. P. Tee, S. S. Ge, Control of state-constrained nonlinear systems using Integral Barrier Lyapunov Functionals, *2012 IEEE 51st IEEE Conference on Decision and Control*, 2012. https://doi.org/10.1109/CDC.2012.6426196
27. K. P. Tee, S. S. Ge, E. H. Tay, Barrier Lyapunov Functions for the control of output-constrained nonlinear systems, *Automatica*, **45** (2009), 918–927. https://doi.org/10.1016/j.automatica.2008.11.017
28. Y. J. Liu, S. C. Tong, C. L. P. Chen, D. J. Li, Adaptive NN control using integral barrier Lyapunov functionals for uncertain nonlinear block-triangular constraint systems, *IEEE T. Cybernetics*, **47** (2017), 3747–3757. https://doi.org/10.1109/TCYB.2016.2581173
29. K. Zhao, Y. D. Song, Z. R. Zhang, Tracking control of MIMO nonlinear systems under full state constraints: A Single-parameter adaptation approach free from feasibility conditions, *Automatica*, **107** (2019), 52–60. https://doi.org/10.1016/j.automatica.2019.05.032
30. L. H. Kong, X. B. Yu, S. Zhang, Neuro-learning-based adaptive control for state-constrained strict-feedback systems with unknown control direction, *ISA Trans.*, **112** (2021), 12–22. https://doi.org/10.1016/j.isatra.2020.12.001

AIMS Press

© 2022 the Author(s), licensee AIMS Press. This is an open access article distributed under the terms of the Creative Commons Attribution License (http://creativecommons.org/licenses/by/4.0)